Available online at www.sciencedirect.com
ScienceDirect
Trans. Nonferrous Met. Soc. China 31(2021) 3591−3601
Transactions of Nonferrous Metals Society of China
www.tnmsc.cn

Selective recovery of Cu(II) through polymer inclusion membranes mediated with 2-aminomethylpyridine derivatives

Xue-jing QIU, Jia TANG, Jun TAN, Hui-ping HU, Xiao-bo JI, Jiu-gang HU

College of Chemistry and Chemical Engineering, Central South University, Changsha 410083, China

Received 24 September 2021; accepted 5 November 2021

Abstract: The Cu(II) separation behaviors with polymer inclusion membranes (PIMs) are explored by modifying 2-aminomethylpyridine derivatives with hydrophobic alkyl chains, including 2-[N-(tert-butyloxycarbonylmethyl)-2-picolyamino]acetate (AMB), N,N-dioctyl-2-aminomethylpyridine (AMD), tert-butyl 2-(N-octyl-2-picolyamino) acetate (AMC), and N,N-didecyl-2-aminomethylpyridine (AME). The transport flux and selectivity of Cu(II) are determined by optimizing composition and structure of carriers and plasticizers. The results show that the hydrophobic modification of 2-aminomethylpyridine derivatives can boost the selective transport of copper ions in PIMs and membrane stability. In the optimum composition of 30 wt.% PVC, 30 wt.% AME, and 40 wt.% NPOE, the initial flux of Cu(II) is 5.8×10^{-6} mol·m^{-2}·s^{-1}. The FT-IR and XPS spectra identify that the alkyl amine functional groups of AME involve in the transport of copper chloride species. The SAXS analysis demonstrates that the generated micro-channels in PIMs induced by the hydrophobic modification of 2-aminomethylpyridine derivatives can contribute to the enhanced Cu(II) flux.

Key words: hydrophobic modification; 2-aminomethylpyridine derivative; polymer inclusion membrane; Cu(II) separation

1 Introduction

Sustainable recovery of Cu(II) from waste liquors is of great significance because of its relative toxic hazardousness and high value [1−3]. Although solvent extraction is the most widely used approach to separate Cu(II) in hydrometallurgical industry, the low concentration of copper(II) will inevitably induce large equipment investment and reagent consumption [4,5]. Recently, the membrane-based separation technology has attracted increasing attention in both industrial applications and wastewater treatments for the separation of inorganic anions or metallic species [6]. Compared with conventional liquid membranes, polymer inclusion membranes (PIMs) offer an attractive alternative due to their excellent stability, selectivity, and mechanical properties [7]. Generally, PIMs are composed of plasticizer and carrier filled between the entangled chains of a polymer, such as poly(vinyl chloride) or cellulose triacetate [8,9]. However, the permeability deterioration still exists in PIMs after several transport cycles owing to their instability caused by the leakage of carrier and plasticizer into aqueous solutions [10].

Although several factors could influence the transport properties and stability of PIMs such as polymer type, plasticizer or carrier, and membrane configurations, the membrane constituents can be one of the most significant variables. CHO et al [11] investigated the influence of different long-chain alkyl alcohols as modifiers on PIM stability. The

Corresponding author: Jiu-gang HU, Tel: +86-13786186961, E-mail: hujiugang@csu.edu.cn; Jun TAN, E-mail: csu_tanjun@163.com
DOI: 10.1016/S1003-6326(21)65750-3

modifier with lower water solubility can provide long-term stability. O'BRYAN et al [12] successfully constructed a semi-interpenetrating crosslinked polymer network containing poly(vinylidene fluoride-co-hexafluoropropylene), poly(ethylene glycol) dimethacrylate and Aliquat 336, which presented good stability for successive transport of thiocyanate. However, these studies mainly focus on the influence of polymer or plasticizer on the transport properties and stability of PIMs, ignoring the effect of carrier molecules on membrane properties.

Compared to primary or tertiary amine ligands, the quaternary amine ligands exhibit higher extraction selectivity and are potentially used for selective transport of targeting species across PIMs. POSPIECH and WALKOWIAK [13] used PIMs with tri-*n*-octylamine or tri-iso-octylamine as carriers to selectively separate Cu(II), Co(II), and Ni(II) from chloride media, and found that the initial flux of PIM with tri-iso-octylamine was higher than that with tri-*n*-octylamine. Similarly, BACZYŃSKA et al [14] suggested that more hydrophilic CTA polymer membranes provide a more expanded and rougher surface for better accessibility of the metal ions. Based on our previous work, it was discovered that tert-butyl-2-(N-octyl-2-picolyamino) acetate exhibited a superior extractability and selectivity of Cu(II) over Ni(II) and Co(II) [15,16]. The high selectivity may be attributed to the structural modification of the aminomethylpyridine molecules with hydrophobic alkyl chain group. However, when these specific carriers were constrained into the polymer matrix, their mobility would be limited and affected the recovery of Cu(II). Therefore, these inspire us to systematically investigate the effect of carrier structure on the flux and transport of Cu(II) in PIMs.

In this work, the recovery of Cu(II) through PVC-based polymer inclusion membranes was explored in which four 2-aminomethylpyridine derivatives with different branches were used as carriers. The Cu(II) transport behaviors were discussed by considering the hydrophobic modification of carriers and the compositions of PIMs. The X-ray photoelectron spectra and small-angle X-ray scatting spectra were employed to elucidate the influence of carrier structure on the microstructural characteristics and transport properties of PIMs.

2 Experimental

2.1 Reagents and chemicals

The 2-aminomethylpyridine was purchased from Sigma-Aldrich and used as carrier precursor without further purification. The base polymer was poly(vinyl chloride) (PVC, Sigma-Aldrich) with an average M_w of ~60000. Tetrahydrofuran was used as a solvent. Dibutyl phthalate (DOP), bis(2-ethylhexyl)adipate (DEHA), or 2-nitrophenyloctyl ether (NPOE) were used as plasticizers of PVC-based PIMs. Copper chloride, ammonium chloride, and hydrochloric acid were provided by Sinopharm, China. The feed phase was 1 mmol/L $CuCl_2$ solution of pH 4.5 and the receiving phase was 2 mol/L NH_4Cl solution of pH 9.

2.2 Synthesis of 2-aminomethylpyridine derivatives

The 2-aminomethylpyridine derivatives used as carriers in PIMs were synthesized according to a similar procedure previously described [15,16]. Taking the synthesis of N,N-didecyl-2-aminomethylpyridine (denoted as AME) as an example, a mixture of 2-aminomethylpyridine (0.048 mol), 1-bromodecane (0.096 mol), triethylamine (0.096 mol), and potassium iodide (0.48 mmol) in ethanol (200 mL) was refluxed for 48 h at 353 K. After cooling to ambient temperature, the precipitate of ammonium salt was filtered off, and the ethanol was evaporated. The liquid residue was extracted with ethyl acetate and washed with saturated sodium chloride. After decantation, ethyl acetate was evaporated. The crude product was purified using a silica gel column to obtain the yellow oil of N,N-didecyl-2-aminomethylpyridine (AME), where the eluent was petroleum ether/ethyl acetate (5:1). The product was identified using ^{1}H NMR spectra (^{1}H NMR (500 Hz, $CDCl_3$): δ: 8.53−8.48 (d, 1H), 7.63 (td, J=7.7, 1H), 7.49 (d, 1H), 7.12 (dd, 1H), 3.70 (s, 2H), 2.47−2.43 (t, 4H), 1.50−1.42 (t, 4H), 1.30 (t, 4H), 1.24 (s, 24H), 0.88 (t, 6H)).

Similarly, 2-[N-(tert-butyloxycarbonylmethyl)-2-picolyamino] acetate (denoted as AMB), tert-butyl 2-(N-octyl-2-picolyamino) acetate (denoted as AMC), and N,N-dioctyl-2-aminomethylpyridine (denoted as AMD) were also synthesized (AMB, δ of ^{1}H NMR (500 Hz, $CDCl_3$): 8.54 (t, 1H),

7.75−7.59 (m, 2H), 7.21–7.10 (m, 1H), 4.02 (d, 2H), 3.49 (s, 4H), 1.46 (s, 18H); AMC, δ of ^{1}H NMR (500 Hz, $CDCl_3$): 8.54 (d, 1H), 7.66 (td, 1H), 7.56 (d, 1H), 7.16 (dd, 1H), 3.93 (s, 2H), 2.31 (s, 2H), 2.64 (m, 2H), 1.54−0.79 (m, 24H); AMD, δ of ^{1}H NMR (500 Hz, $CDCl_3$): 8.53 (d, 1H), 7.66 (td, 1H), 7.53 (m, 1H), 7.17 (dd, 1H), 3.73 (s, 2H), 2.47 (s, 4H), 1.67−1.26 (m, 24H), 0.89 (t, 6H)). The molecular structures of four 2-aminomethylpyridine derivatives are shown in Fig. 1.

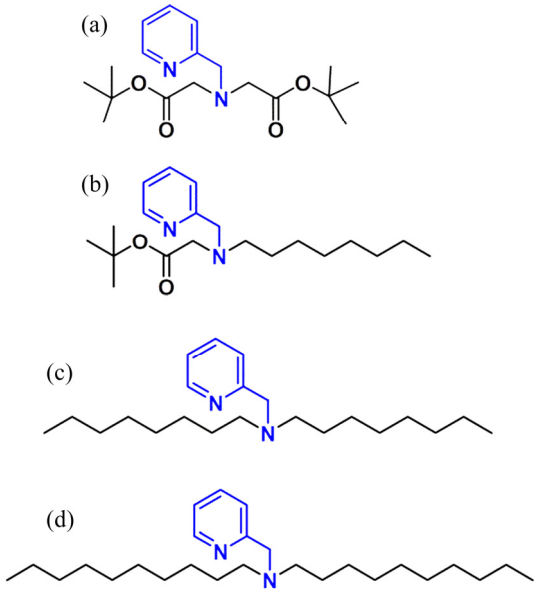

Fig. 1 Molecular structures of AMB (a), AMC (b), AMD (c), and AME (d)

2.3 Preparation of PIMs

PIMs were prepared using the solvent evaporation method [16]. Typically, 0.3 g membrane components, including PVC polymer, and DOP, DEHA or NPOE as a plasticizer, as well as 2-aminomethylpyridine derivatives (AMB, AMC, AMD or AME) as the carrier, were dissolved in 5 mL tetrahydrofuran under stirring for 2 h. Then, the mixed solution was poured into a Petri dish with a 6.5 cm in diameter and covered with filter tissue. Tetrahydrofuran was allowed to evaporate for 12 h to form a transparent and flexible polymer inclusion membrane. The resulting PIMs were carefully peeled off and used for Cu(II) transport experiments.

2.4 Cu(II) transport experiments

Transport experiments were carried out with a two-compartment cell in a water bath of 30 °C. The PIM was sandwiched between two compartments. The flow rate of both feed and receiving solutions was set at 100 mL/min with peristaltic pumps. The volume of each solution was 80 mL. The effective membrane surface area was 1.256×10^{-3} m^2. The transport behaviors of metal ions were determined in 0.5 mL solutions aliquoted from feed and receiving compartments at each 1 h for 6 h, respectively. For the successive transport test, the fresh feed and receiving solutions were used after each cycle. The metal concentration was analyzed by flame atomic absorption spectroscopy (TAS-990F, China).

The recovery (R, %) is defined with the ratio of Cu(II) concentration in receiving solutions to that in feed solution. The kinetics of transport through PIMs is described by the following equation:

$$\ln\frac{c}{c_0}=-kt \tag{1}$$

where c_0 and c are the concentrations of the metal ions (mg/L) in the feed solution at the initial time and the desired time; k (s^{-1}) is the kinetic rate constant; t (s) is the transport time.

The permeability coefficient (P) is calculated as follows:

$$P=\frac{V}{A}k \tag{2}$$

where V is the volume of the feed solution (0.08 L); A is the effective area of PIM (1.256×10^{-3} m^2). The initial flux (J_0, mol·m^{-2}·s^{-1}) is calculated from P values by the following equation:

$$J_0=P\cdot c_0 \tag{3}$$

2.5 Structural characterization

The FT-IR spectra of PIMs were collected by using a Nicolet 6700 Fourier-Transform Infrared Spectrophotometer (Thermo Scientific, USA). Hydrophobicity of the membrane surfaces was evaluated with contact angle measurement on a Teclis T2010 instrument equipped with a video system. X-ray photoelectron spectra were measured on a 250Xi spectrometer (Thermo Scientific, USA) with Al K_α X-ray source (1486.6 eV of protons) and a high vacuum of 10^{-8} Pa. XPS spectra were corrected and analyzed with the Avantage 5.52 software. The small-angle X-ray scattering (SAXS) data of PIMs were collected at beam line 1W2A at Beijing Synchrotron Radiation Facility (China). The storage ring was operated at 2.5 GeV with a current about 80 mA. The 2D scattering patterns were

integrated into 1D scattered intensities (q) as a function of the magnitude of the scattering vector $q=(4\pi/\lambda)\sin(\theta/2)$, where θ and λ are the total scattering angle and the wavelength of the incident beam, respectively. The SAXS data were interpreted by the GIFT method to obtain pair-distance distribution functions (PDDFs) and provide information on the shape and the size of the membrane components.

3 Results and discussion

3.1 Effect of carrier structure on Cu(II) transport

The membrane constituents can seriously affect their mechanical stability and transport performance of PIMs. As shown in Fig. 2, when the carrier content is fixed at 30 wt.% and no plasticizer NPOE is added, the PIMs with AMB or AMC are rigid, but the PIMs become flexible and present a slight increase of transport ability after adding more hydrophobic AMD or AME, suggesting that the hydrophobic 2-aminomethylpyridine derivatives have a potential plasticizing effect. After adding NPOE, compared with the PIMs with AMB or AMC, the initial flux (J_0) and recovery of Cu(II) evidently increase in the presence of hydrophobic AMD or AME, indicating the synergistic plasticizing effect between 2-aminomethylpyridine derivatives and NPOE. Moreover, the increase of NPOE content leads to an improvement in the initial flux and recovery of copper ions. This phenomenon may be attributed to the increasing mobility of transporting species by reducing the intermolecular forces between polymer chains with the plasticizer NPOE molecules. When NPOE content is beyond 40 wt.%, the PIMs are too sticky and have a poor mechanical strength for transport experiments. While fixing the PVC content at 30 wt.% and increasing the NPOE content from 30 to 40 wt.%, the initial flux and recovery of copper ions still increase even though the carrier content accordingly decreases (Figs. 2(c, d)), which indicates the synergistic plasticizing effect between NPOE and 2-aminomethylpyridine derivatives. Consequently, the PIMs with the composition of

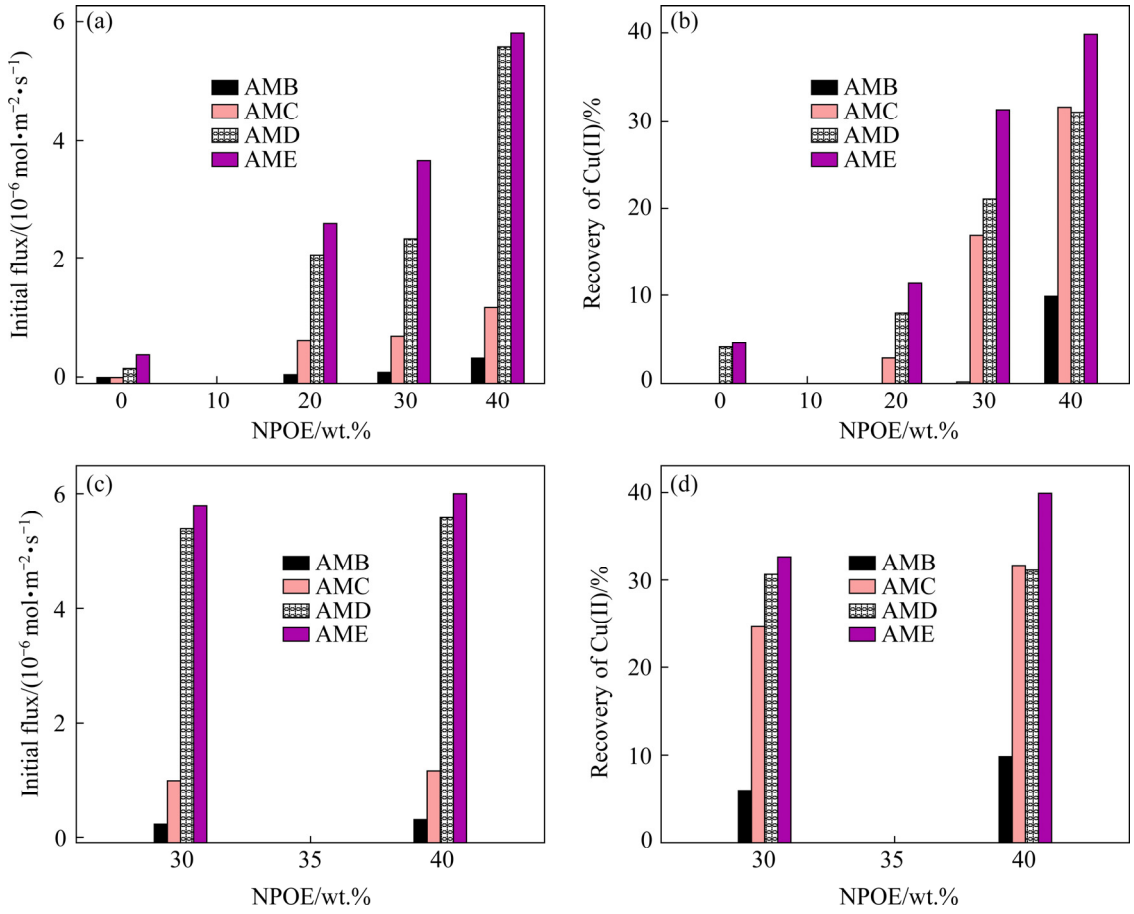

Fig. 2 Effect of membrane compositions on initial flux (a, c) and recovery of Cu(II) (b, d) in PIMs with different carriers: (a, b) Fixing carrier content at 30 wt.%; (c, d) Fixing PVC content at 30 wt.%

30 wt.% PVC, 40 wt.% NPOE, and 30 wt.% carriers are used to further evaluate the effect of the molecular structure of four 2-aminomethylpyridine derivatives on Cu(II) transport.

Under the optimized membrane compositions, the structural effect of the carriers on Cu(II) flux is shown in Fig. 3(a). It is discovered that PIMs containing more hydrophobic AME have higher transport flux. The Cu(II) flux in the PIMs containing 2-aminomethylpyridine derivatives increases in the order of AMB < AMC < AMD < AME with J_0 values of $(0.31\pm0.02)\times10^{-6}$, $(1.17\pm0.08)\times10^{-6}$, $(5.58\pm0.05)\times10^{-6}$, and $(5.82\pm0.03)\times10^{-6}$ mol·m^{-2}·s^{-1}, respectively. It can be concluded that the replacement of the hydrophilic ester groups with a hydrophobic alkyl chain of the carrier can improve the transport flux of copper ions in PIMs, where PIM containing AME exhibits the better transportability towards Cu(II) than the other three carriers. Although the previous extraction experiments indicated that the 2-aminomethylpyridine derivatives with hydrophilic ester groups more easily coordinate with copper ions [17], the transport results indicate that the Cu(II) flux is highly dependent on the molecular structure and hydrophobicity of 2-aminomethylpyridine derivatives. In the polyvinyl chloride matrix, the compatibility between transported Cu(II) species and plasticizer molecules should be improved when increasing the alkyl chain of 2-aminomethylpyridine derivatives, thus benefiting the mass transfer in PIMs. Besides, the carrier molecules also modify the surface properties of PIMs. As shown in Fig. 3(b), the contact angle of PIMs containing AMB, AMC, AMD or AME is (60.25±0.13)°, (62.61±0.21)°, (68.15±0.17)°, and (72.54±0.15)°, respectively, which indicates that the modification of 2-aminomethylpyridine derivatives with long alkyl chains promotes the hydrophobicity of the PIM surface [18,19].

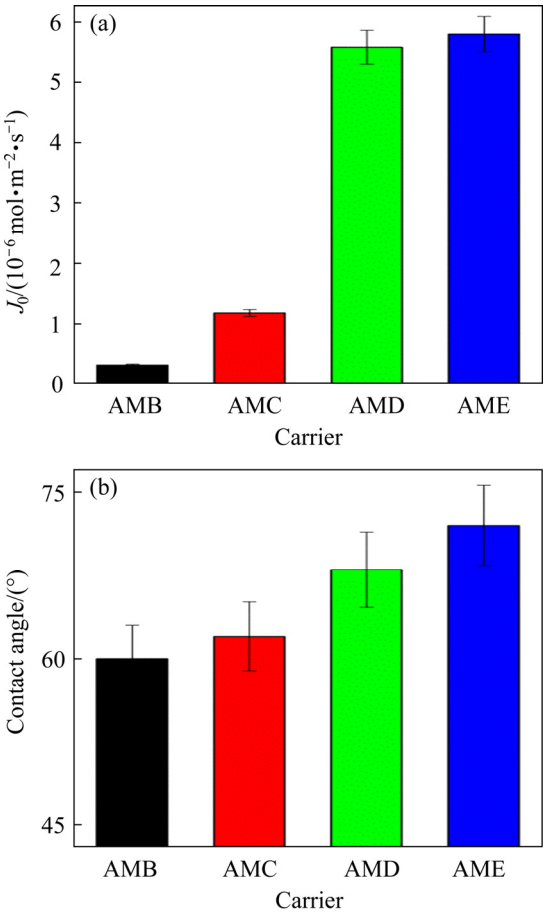

Fig. 3 Effect of carrier type on Cu(II) flux (J_0) (a) and surface hydrophobicity (b) of PIMs with 30 wt.% carrier, 30 wt.% PVC, and 40 wt.% NPOE

3.2 Effect of plasticizer on Cu(II) transport

As discussed above, the plasticizer molecules need to be added in the PIM matrix to improve the flexibility and the component compatibility. Therefore, the influence of plasticizer types in PIMs on the initial flux of Cu(II) is examined. The results in Fig. 4 show that the Cu(II) flux of PIMs containing 30 wt.% AME as a carrier is 5.8×10^{-6}, 3.31×10^{-6}, and 2.76×10^{-6} mol·m^{-2}·s^{-1} when 40 wt.% NPOE, DOP, or DEHA is used as the plasticizer, respectively. This phenomenon is also observed for the PIMs containing other three 2-aminomethylpyridine derivatives, indicating that NPOE is more efficient than DOP or DEHA to improve the Cu(II) transport. This behavior could be attributed to the larger dielectric constant of NPOE molecules, which could modify the mobility of Cu(II) complexes formed in the membrane matrix [20]. Moreover, no matter which plasticizer is used, it can be observed that Cu(II) flux of PIMs containing AME is significantly higher than that of the other three 2-aminomethylpyridine derivatives. The Cu(II) flux across PIMs containing different carriers increases in the same order of AMB < AMC < AMD < AME under the same composition proportion. These results further verify that the hydrophobic modification of the carrier molecules can improve the flux of the PIMs.

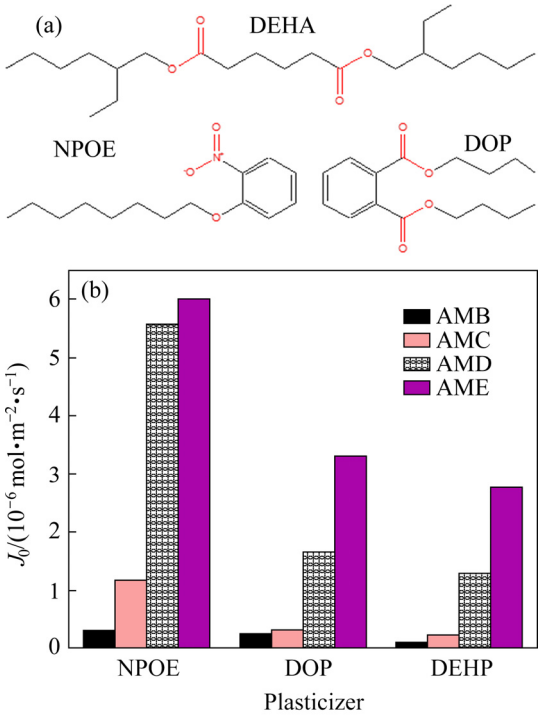

Fig. 4 Molecular structure of plasticizers (a) and their effect on Cu(II) flux (J_0) of PIMs with 30 wt.% carrier, 30 wt.% PVC, and 40 wt.% plasticizer (b)

3.3 Selective transport of metal ions

The selective transports of Cu(II), Ni(II), and Co(II) through PIMs on the corresponding initial flux containing each of the four carriers are performed. As shown in Fig. 5, the flux values of Cu(II) for PIMs containing AMB, AMC, AMD, and AME is 1.42×10^{-6}, 2.52×10^{-6}, 6.62×10^{-6} and 6.81×10^{-6} mol·m^{-2}·s^{-1}. It is interesting to observe that the initial flux is increased in the competitive transport process, which may result from the formation of extractable Cu(II) species induced by the addition of $NiCl_2$ and $CoCl_2$. Accordingly, the membrane containing AMD or AME ligand has the higher transport value than other two ligands due to its greater hydrophobic nature relative to AMB and AMC [21]. And again, the flux values (6.81×10^{-6}, 1.35×10^{-6}, and 1.23×10^{-6} mol·m^{-2}·s^{-1}) of the PIM with AME to Cu(II), Co(II), and Ni(II) are higher than those of the other three carriers, illustrating that the hydrophobic modification of the carrier molecules can further improve the selective transport of Cu(II) over Co(II) and Ni(II).

3.4 Stability test of PIMs

The stability of PIMs containing AMC, AMD or AME as the carrier is investigated in successive five cycles. Because of the low initial flux, the PIM containing AMB is not further considered. As displayed in Fig. 6, the initial flux of PIM containing AME is always higher than that of PIM containing AMC or AMD during the cycle tests. After five cycles, the initial flux of PIM containing AME slightly decreases from 5.85×10^{-6} to 5.53×10^{-6} mol·m^{-2}·s^{-1}, whereas the flux of PIM containing AMC decreases from 1.17×10^{-6} to 0.94×10^{-6} mol·m^{-2}·s^{-1}. The decrease in the initial flux of PIMs may be caused by the leaching of the carrier with lower hydrophobicity. The flux retention rate is about 80.3%, 93.8% and 94.5% for PIMs with AMC, AMD or AME, respectively, implying that the flux and stability are improved by increasing the length of the alkyl chain of the carrier used. Therefore, the hydrophobic

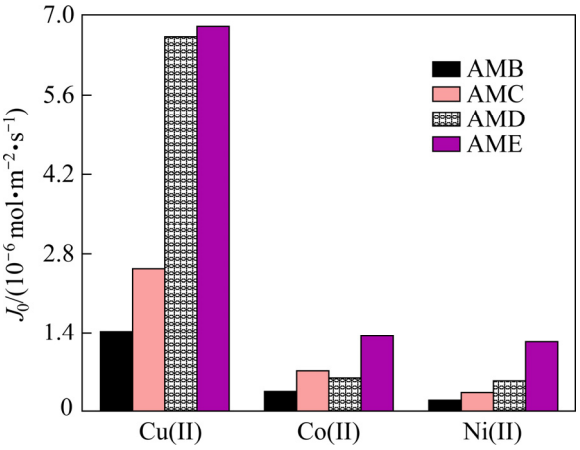

Fig. 5 Competitive transport and initial flux (J_0) of Cu(II), Co(II), and Ni(II) through PIMs with different carriers (1 mmol/L each of Cu(II), Co(II), and Ni(II); pH=4.5)

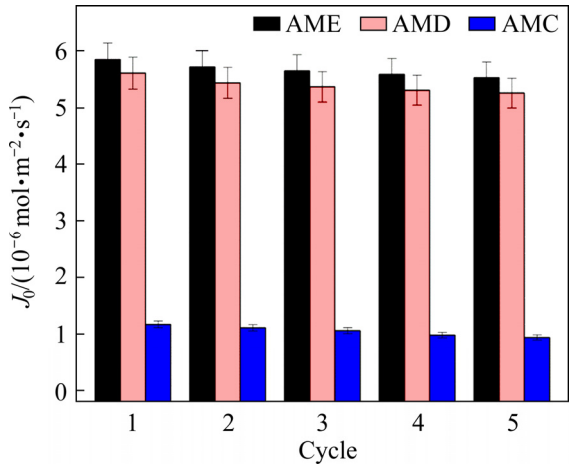

Fig. 6 Initial flux of PIMs containing different carriers during five cycles

modification of 2-aminomethylpyridine derivatives is also beneficial to the stability of the polymer inclusion membrane.

3.5 Transport mechanism of Cu(II)

The FT-IR spectra of PIM containing AME before and after reacting with Cu(II) are exhibited in Fig. 7. The characteristic peaks located at 1527 and 1165 cm^{-1} correspond to C—N and C—O—C bonds of NPOE molecules. The narrow peaks at 1465 and 1431 cm^{-1} are assigned to its C—H groups. The peaks near 1353 and 1569 cm^{-1} are attributed to the stretching vibrations of C—N and C═N from the carrier molecules. Compared with the fresh PIM containing AME, it can be observed that the stretching vibrations of C═N slightly blue shift after Cu(II) transport [22], confirming that AME is coordinated with Cu(II) ions through pyridine N atoms. Based on the FT-IR results, there are only weak interactions between constituents and no formation of covalent bonds [23].

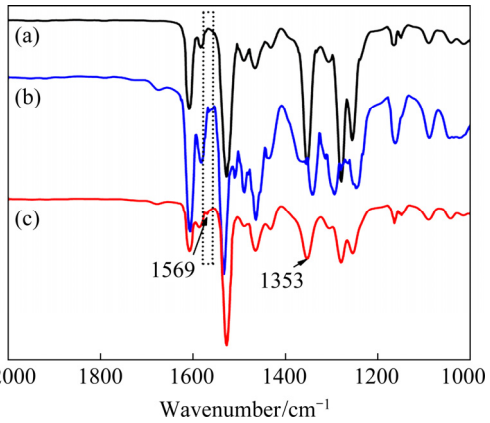

Fig. 7 FT-IR spectra of blank membrane without AME (a), PIM with AME before Cu(II) transport (b), and PIM with AME after Cu(II) transport (c)

The chemical interaction of PIMs containing AME is further examined by XPS before and after reacting with Cu(II) species. The XPS spectra wide scans, N 1s and Cl 2p spectra of PIMs are presented in Fig. 8. The photoelectron lines of N 1s and Cl 2p

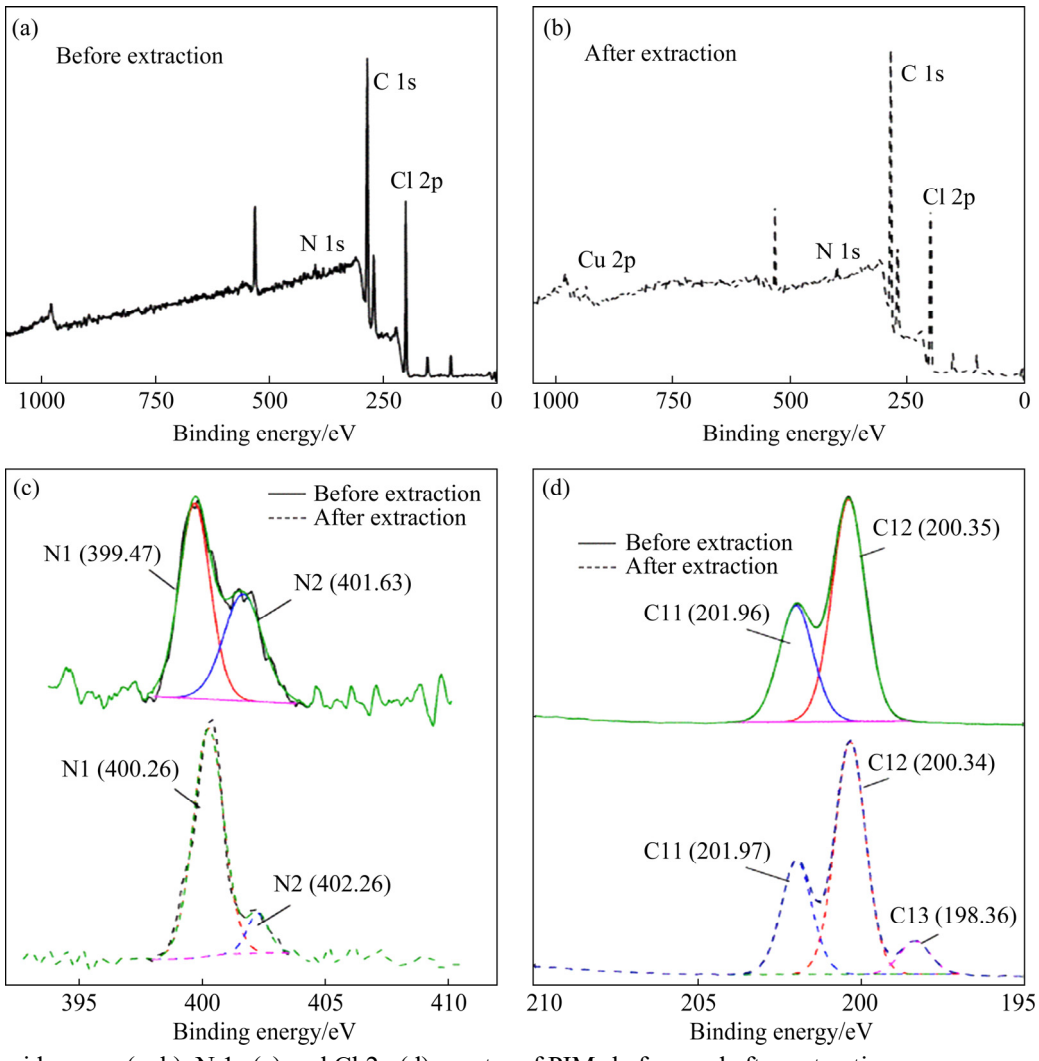

Fig. 8 XPS wide scans (a, b), N 1s (c) and Cl 2p (d) spectra of PIMs before and after extraction

of PIMs are identified from the survey spectra before and after Cu(II) transport. The presence of Cu 2p peak indicates that the copper species are extracted into PIMs (Figs. 8(a, b)). From the N 1s core-level spectrum (Fig. 8(c)), two characteristic peaks of N 1s from the AME molecules are observed and the binding peaks at 399.47 eV and 401.63 eV originate from the nitrogen atoms in the C═N groups of pyridine ring and C—N groups of the aliphatic amine, respectively. After extraction of Cu(II) into PIMs, the respective binding energies of the pyridine N 1s and the aliphatic N 1s are correspondingly shifted by 0.79 and 0.63 eV to the higher direction of the high binding energy. Notably, the peak intensity of aliphatic N 1s has been depressed after reacting with Cu(II), indicating that the copper species can be extracted by the aliphatic amine functional group. A new peak at 198.36 eV for Cu(II)-loaded PIMs can be observed from the Cl 2p spectrum (Fig. 8(d)), verifying that copper species containing chloride ions can be transported across the PIM by the amine functional group of AME [24,25].

The SAXS curves of the PVC + NPOE membrane are collected in the absence and presence of different 2-aminomethylpyridine derivatives as carriers. The corresponding normalized SAXS and the PDDFs curves are shown in Fig. 9. Figure 9(a) shows a series of 2D scattering patterns of PIMs. It can be clearly seen that the brightness of the scattering pattern increases with increasing the hydrophobicity of 2-aminomethylpyridine derivatives. Moreover, the brightness of the scattering pattern of PIM decreases after reacting with Cu(II),

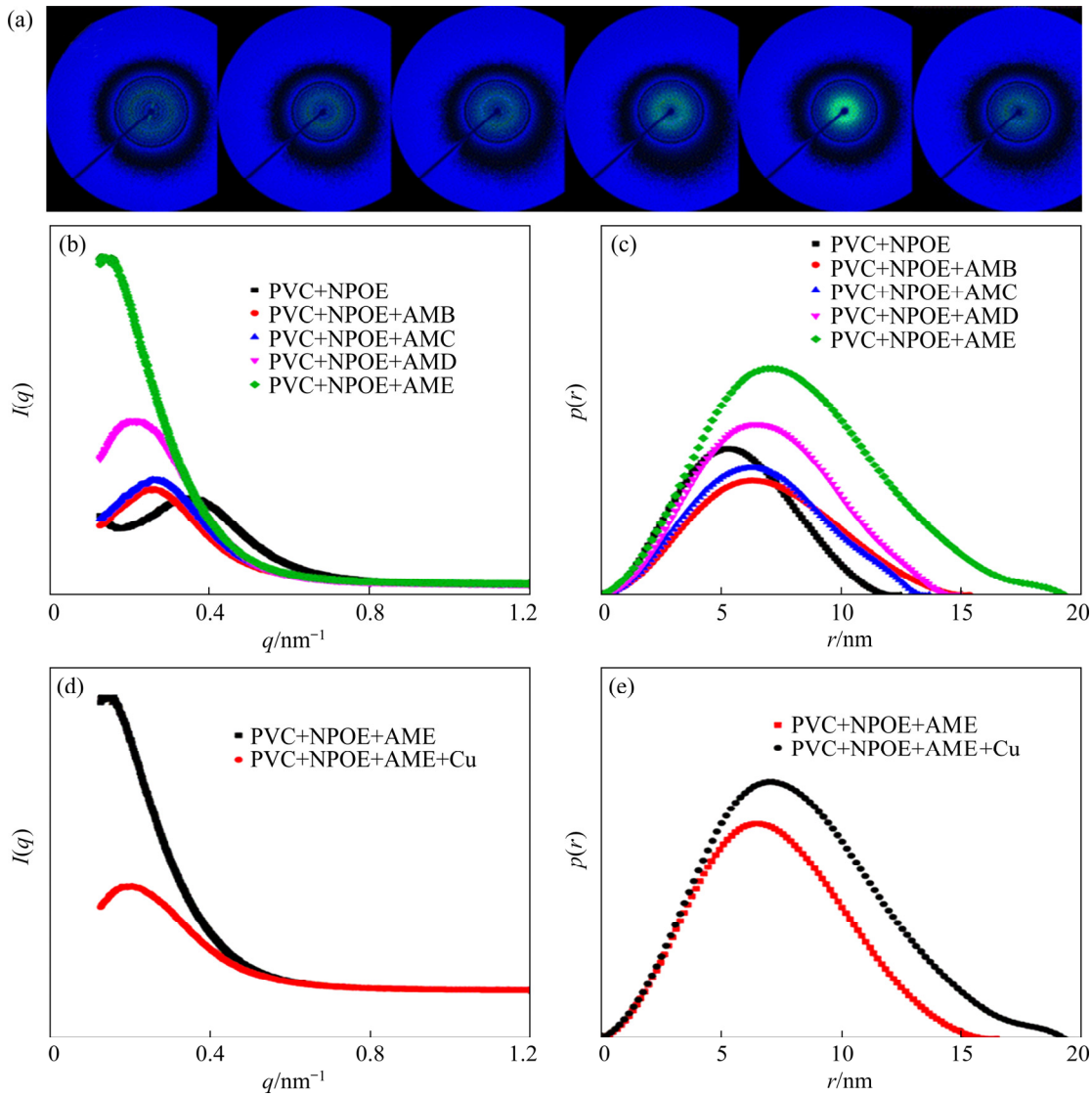

Fig. 9 2D scattering patterns of PIMs without carrier and with AMB, AMC, AMD, or AME, and PIMs with AME after loading Cu(II) (a) corresponding normalized SAXS curves (b, d), and PDDFs (c, e)

demonstrating the formation of liquid micro-domains in PIMs after adding hydrophobic 2-aminomethylpyridine derivatives. As shown in Fig. 9(b), the peak of SAXS curves moves to a lower q value and the intensity increases toward the primary beam position [26,27], suggesting that the liquid micro-domains in PIMs increase because of the increased hydrophobicity of 2-aminomethylpyridine derivatives [28]. The GIFT-generated $p(r)$ functions shown in Fig. 9(c) present the change of the spherical aggregate structure in PIMs with different hydrophobic carriers. Increasing the hydrophobicity of 2-aminomethylpyridine derivatives in PIMs can result in a shift of the peak position and elongation of the function to higher r. In the view of the results described above, there appear some narrow micro-channels and cracks in the PVC + NPOE membrane without any carriers due to the plasticization effect of NPOE. Moreover, the generated micro-channels in PIMs can be evidently extended and expanded after adding 2-aminomethylpyridine derivatives. Therefore, increasing the hydrophobicity of the carrier is beneficial to the further increase of the micro-domains and channels. In addition, Figs. 9(d, e) show that the scattering peak position slightly moves to the lower scattering vector value after reacting with Cu(II). This slight shift is related to the coordination between AME and Cu(II), which causes a slight contraction of the liquid micro-domains of PIMs [29,30].

4 Conclusions

(1) The replacement of the hydrophilic ester groups with a hydrophobic alkyl chain of 2-aminomethylpyridine derivatives can improve the transport flux of copper ions in PIMs.

(2) The higher Cu(II) flux and better stability of PIM containing AME could result from the large surface hydrophobicity and good component compatibility in the membrane matrix.

(3) The FT-IR and XPS spectra of PIMs identify that the alkyl amine functional groups of AME involve in the transport of Cu(II) species containing chloride ions. The SAXS results reveal that the formation of micro-domains and channels induced by hydrophobic 2-aminomethylpyridine derivatives can contribute to boosting the transport flux of Cu(II) across PIMs.

Acknowledgments

The authors are grateful for the financial supports from the National Key R&D Program of China (No. 2019YFC1907801), National Natural Science Foundation of China (No. 52174286), Hunan Provincial Science and Technology Plan Project, China (No. 2019JJ30031), and Innovation-Driven of Central South University, China (No. 2020CX007).

References

[1] ZHAN You-cai, LUO Xu-biao, NIE Shang-shan, HUANG Yin-ning, TU Xin-man, LUO Sheng-lian. Selective separation of Cu(II) from aqueous solution with a novel Cu(II) surface magnetic ion-imprinted polymer [J]. Industrial & Engineering Chemistry Research, 2011, 50: 6355−6361.

[2] YIN Wan-zhong, SUN Qian-yu, LI Dong, TANG Yuan, FU Ya-feng, YAO Jin. Mechanism and application on sulphidizing flotation of copper oxide with combined collectors [J]. Transactions of Nonferrous Metals Society of China, 2019, 29: 178−185.

[3] SHI Mei-qing, MIN Xiao-bo, SHEN Chen, CHAI Li-yuan, KE Yong, YAN Xu, LIANG Yan-jie. Separation and recovery of copper in Cu−As-bearing copper electrorefining black slime by oxidation acid leaching and sulfide precipitation [J]. Transactions of Nonferrous Metals Society of China, 2021, 31: 1103−1112.

[4] SOEEZI A, ABDOLLAHI H, SHAFAEI S Z, RAHIMI E. Extraction and stripping of Cu and Ni from synthetic and industrial solutions of Sarcheshmeh copper mine containing Cu, Ni, Fe and Zn ions [J]. Transactions of Nonferrous Metals Society of China, 2020, 30: 518−534.

[5] HAJMOHAMMADI H, JAFARI A H, NASAB M E. Scandium recovery from raffinate copper leach solution as potential new source with ion exchange method [J]. Transactions of Nonferrous Metals Society of China, 2020, 30: 3103−3113.

[6] ALMEIDA M, CATTRALL R W, KOLEV S D. Polymer inclusion membranes (PIMs) in chemical analysis—A review [J]. Analytica Chimica Acta, 2017, 987: 1−14.

[7] TURGUT H I, EYUPOGLU V, KUMBASAR R A, SISMAN I. Alkyl chain length dependent Cr(VI) transport by polymer inclusion membrane using room temperature ionic liquids as carrier and PVDF-co-HFP as polymer matrix [J]. Separation and Purification Technology, 2017, 175: 406−417.

[8] WANG Duo, HU Jiu-gang, LI Ya, FU Ming-bo, LIU Da-biao, CHEN Qi-yuan. Evidence on the 2-nitrophenyl octyl ether (NPOE) facilitating copper(II) transport through polymer inclusion membranes [J]. Journal of Membrane Science, 2016, 501: 228−235.

[9] KAMRAN H H, IRANNAJAD M, MARIA S A. Germanium transport across supported liquid membrane with Cyanex 923: Mathematical modeling [J]. Transactions of Nonferrous Metals Society of China, 2019, 29: 1956−1966.

[10] KAGAYA S, RYOKAN Y, CATTRALL R W, KOLEV S D. Stability studies of poly(vinyl chloride)-based polymer inclusion membranes containing Aliquat 336 as a carrier [J]. Separation and Purification Technology, 2012, 101: 69−75.

[11] CHO Y, XU Chun-lan, CATTRALL R W, KOLEV S D. A polymer inclusion membrane for extracting thiocyanate from weakly alkaline solutions [J]. Journal of Membrane Science, 2011, 367: 85−90.

[12] O'BRYAN Y, TRUONG Y B, CATTRALL R W, KYRATZIS I L, KOLEV S D. A new generation of highly stable and permeable polymer inclusion membranes (PIMs) with their carrier immobilized in a crosslinked semi-interpenetrating polymer network: Application to the transport of thiocyanate [J]. Journal Membrane Science, 2017, 529: 55−62.

[13] POSPIECH B, WALKOWIAK W. Separation of copper(II), cobalt(II) and nickel(II) from chloride solutions by polymer inclusion membranes [J]. Separation and Purification Technology, 2007, 57: 461−465.

[14] BACZYŃSKA M, WASZAK M, NOWICKI M, PRZĄDKA D, BORYSIAK S, REGEL-ROSOCKA M. Characterization of polymer inclusion membranes (PIMs) containing phosphonium ionic liquids as Zn(II) carriers [J]. Industrial & Engineering Chemistry Research, 2018, 57: 5070−5082.

[15] YANG Jin-peng, HU Hui-ping, CHENG Ze-ying, QIU Xue-jing, WANG Cai-xia. Structural insights into the coordination and selective extraction of copper(II) by tertiary amine ligands derived from 2-aminomethylpyridine [J]. Polyhedron, 2017, 128: 76−84.

[16] CHENG Ze-ying, HU Hui-ping, YANG Jin-peng, QIU Xue-jing, WANG Cai-xia, Ji Guang-fu. Synthesis, structure and DFT calculations of a novel copper(II) complex based on tert-butyl 2-[N-(tert-butyloxycarbonylmethyl)-2-picolyamino] acetate [J]. Chinese Journal of Structural Chemistry, 2017, 36: 795−804.

[17] QIU Xue-jing, HU Hui-ping, YANG Jin-peng, WANG Cai-xia, CHENG Ze-ying, JI Guang-fu. Selective removal of copper from simulated nickel electrolyte by polystyrene-supported 2-aminomethylpyridine chelating resin [J]. Chemical Papers, 2018, 72: 2071−2085.

[18] VERA R, GELDE L, ANTICÓ E, de MARTÍNEZ Yuso M V, BENAVENTE J, FONTÀS C. Tuning physicochemical, electrochemical and transport characteristics of polymer inclusion membrane by varying the counter−anion of the ionic liquid Aliquat 336 [J]. Journal of Membrane Science, 2017, 529: 87−94.

[19] ZIOUI D, AROUS O, MAMERI N, KERDJOUDJ H, SEBASTIAN M S, VILAS J L, NUNES-PEREIRA J, LANCEROS-MENDEZ S. Membranes based on polymer miscibility for selective transport and separation of metallic ions [J]. Journal of Hazardous Materials, 2017, 336: 188−194.

[20] ALMEIDA S, CATTRALL R W, KOLEV S D. Recent trends in extraction and transport of metal ions using polymer inclusion membranes (PIMs) [J]. Journal of Membrane Science, 2012, 415−416: 9−23.

[21] QIU Xue-jing, HU Hui-ping, YANG Jin-peng, CHENG Ze-ying, JI Guang-fu. A theoretical investigation on the selective extraction of Cu(II) from Ni(II) by 2-aminomethylpyridine derivatives: A DFT study [J]. Polyhedron, 2019, 157: 200−207.

[22] LI Ji-yuan, HU Hui-ping, ZHU Shan, HU Fang, WANG Yong-xi. The coordination structure of the extracted nickel(II) complex with a synergistic mixture containing dinonylnaphthalene sulfonic acid and 2-ethylhexyl 4-pyridinecarboxylate ester [J]. Dalton Transactions, 2017, 46: 1075−1082.

[23] SAF A Ö, ALPAYDIN S, COSKUN A, ERSOZ M. Selective transport and removal of Cr(VI) through polymer inclusion membrane containing 5-(4-phenoxyphenyl)-6H-1,3,4-thiadiazin-2-amine as a carrier [J]. Journal of Membrane Science, 2011, 377: 241−248.

[24] QIU Xue-jing, HU Hui-ping, YANG Jin-peng, WANG Cai-xia, CHENG Ze-ying. Removal of trace copper from simulated nickel electrolytes using a new chelating resin [J]. Hydrometallurgy, 2018, 180: 121−131.

[25] YAO Li-wei, MIN Xiao-bo, XU Hui, KE Yong, WANG Yun-yan, LIN Zhang, LIANG Yan-jie, LIU De-gang, XU Qiu-jing, HE Yu-yang. Physicochemical and environmental properties of arsenic sulfide sludge from copper and lead−zinc smelter [J]. Transactions of Nonferrous Metals Society of China, 2020, 30: 1943−1955.

[26] ELLIS R, ANDERSON T, ANTONIO M, BRAATZ A, NILSSON M. A SAXS study of aggregation in the synergistic TBP−HDBP solvent extraction system [J]. Journal of Physical Chemistry B, 2013, 117: 5916−5924.

[27] HUANG Ting, WANG Yong-xi, HU Hui-ping, HU Fang, LUO Yu-qing, LIU Shi-jun. Phase separation in solvent extraction of cobalt from acidic sulfate solution using synergistic mixture containing dinonylnaphthalene sulfonic acid and 2-ethylhexyl 4-pyridinecarboxylate ester [J]. Transactions of Nonferrous Metals Society of China, 2019, 29: 1107−1116.

[28] NUNES S, BEHZAD A, HOOGHAN B, SOUGRAT R, KARUNAKARAN M, PRADEEP N, VAINIO U, PEINEMANN K. Switchable pH-responsive polymeric membranes prepared via block copolymer micelle assembly [J]. Acs Nano, 2011, 5: 3516−3522.

[29] SEL O, Azais T, MARECHAL M, GEBEL G, LABERTY-ROBERT C, SANCHEZ C. Sulfonic and phosphonic acid and bifunctional organic-inorganic hybrid membranes and their proton conduction properties [J]. Chemistry−An Asian Journal, 2011, 6: 2992−3000.

[30] ELLIS R J. Critical exponents for solvent extraction resolved using SAXS [J]. Journal of Physical Chemistry B, 2014, 118: 315−322.

2-氨甲基吡啶衍生物聚合物包合膜选择性回收 Cu(II)

邱雪景，汤 佳，谭 军，胡慧萍，纪效波，胡久刚

中南大学 化学化工学院，长沙 410083

摘 要：以不同 2-氨甲基吡啶类衍生物(N,N-二(叔丁氧羰基亚甲基)-2-氨甲基吡啶、N,N-二辛基-2-氨甲基吡啶、N-叔氧羰基亚甲基-N-辛基-2-氨甲基吡啶、N,N-二癸基-2-氨甲基吡啶)为载体，制备以聚氯乙烯(PVC)为膜基材的系列聚合物包容膜(PIM)；通过优化载体分子结构和塑化剂类型，考察聚合物包容膜的铜离子渗透通量和分离选择性。结果表明：含有长碳链的疏水性吡啶类衍生物有助于提高铜离子传质通量和膜的稳定性。在 PVC 含量为 30% (质量分数)， N,N-二癸基-2-氨甲基吡啶为 30%(质量分数)，塑化剂为 40% (质量分数)时，铜离子的渗透通量可达 5.8×10^{-6} $mol\cdot m^{-2}\cdot s^{-1}$。FT-IR 和 XPS 分析结果表明，N,N-二癸基-2-氨甲基吡啶上的氨基官能团参与铜离子的配位，SAXS 分析证实 2-氨甲基吡啶类衍生物的疏水性改性有利于膜中微通道的形成，从而促进铜离子在膜内的传质。

关键词：疏水性改性；2-氨甲基吡啶类衍生物；聚合物包容膜；铜离子分离

(Edited by Bing YANG)